Alvarez-Tirado *et al. Energy Mater* 2023;3:300003
DOI: 10.20517/energymater.2022.59

Energy Materials

Article

Open Access

Check for updates

Design of highly conductive iongel soft solid electrolytes for Li-O_2 batteries

Marta Alvarez-Tirado[1,2,4], Laurent Castro[2], Gregorio Guzmán-González[1,5], Aurélie Guéguen[2], Liliana C. Tomé[1,6], David Mecerreyes[1,3,*]

[1]POLYMAT University of the Basque Country UPV/EHU, Donostia-San Sebastian 20018, Spain.
[2]Toyota Motor Europe Research & Development 1, Advanced Material Research, Battery & Fuel Cell, Zaventem B-1930, Belgium.
[3]Ikerbasque, Basque Foundation for Science, Bilbao E-48011, Spain.
[4]Present address: CIDETEC, Basque Research and Technology Alliance (BRTA), Donostia-San Sebastián 20014, Spain.
[5]Present address: Departamento de Química, Universidad Autónoma Metropolitana-Iztapalapa, México City 09340, México.
[6]Present address: LAQV-REQUIMTE, Department of Chemistry, NOVA School of Science and Technology, FCT NOVA, Universidade NOVA de Lisboa, 2829-516 Caparica, Portugal.

[*]**Correspondence to:** Dr. David Mecerreyes, POLYMAT University of the Basque Country UPV/EHU, Joxe Mari Korta Building, Avenida Tolosa 72, Donostia-San Sebastian 20018, Spain. E-mail: david.mecerreyes@ehu.eus

How to cite this article: Alvarez-Tirado M, Castro L, Guzmán-González G, Guéguen A, Tomé LC, Mecerreyes D. Design of highly conductive iongel soft solid electrolytes for Li-O_2 batteries. *Energy Mater* 2023;3:300003. https://dx.doi.org/10.20517/energymater.2022.59

Received: 29 Sep 2022 **First Decision:** 11 Nov 2022 **Revised:** 23 Dec 2022 **Accepted:** 11 Jan 2023 **Published:** 30 Jan 2023

Academic Editors: Yuping Wu, Elie Paillard **Copy Editor:** Fangling Lan **Production Editor:** Fangling Lan

Abstract

Li-O_2 batteries show high energy storage potential, but there remain many material challenges that must be solved to fully develop them into a robust technology. The reactivity of the electrolyte against lithium metal as the anode or with oxygen superoxide radicals in the cathode is the main problem that may be alleviated by the use of ionic liquids and solid electrolytes. In this work, iongel solid flexible electrolytes with facile preparation are designed based on five variations of the successful N,N-diethyl-N-methyl-N-(2-methoxyethyl)ammonium bis(trifluoromethanesulfonyl)imide ionic liquid. These iongels show an outstanding ionic conductivity of 7.8×10^{-3} S·cm^{-1} at 25 °C, excellent performance against lithium metal and reduced dendritic growth, even at a high current density rate of 2 mA·cm^{-2}. Tests on Li-O_2 cells show a 100% capacity retention for 25 cycles with limited capacity. Hence, this work provides a plausible pathway to tackle the design of effective lithium protection methods and efficient solid electrolytes for Li-O_2 batteries.

Keywords: Polymer electrolytes, iongels, ionic liquids, Li-O_2 batteries, lithium metal batteries, solid-state batteries

INTRODUCTION

Despite all the efforts of the research community in recent decades, the commercialization of high-energy-density Li-O_2 batteries is still far from being realized. One of the major problems of this technology is finding an electrolyte material that can simultaneously provide lithium metal protection and stability against highly reactive oxygen species (i.e., superoxide) so that the lifespan of Li-O_2 cells can be prolonged[1,2]. Technologies based on interfacial chemistry regulation (i.e., the stability of the solid electrolyte interphase, SEI), nanostructured-based solutions (i.e., aligned nanochannels to delay dendrite growth) or the development of solid electrolytes are plausible strategies to enhance the Li-O_2 cell lifetime by protecting the metal anode and reducing safety concerns[3]. For example, Chen *et al.* developed an effective artificial SEI film by impregnating lithium metal with triethylamine trihydrofluoride under controlled conditions[4]. This process forms a uniform layer of LiF, which is able to minimize side reactions with the electrolyte and lithium dendrite growth in both symmetrical and Li^0/$LiFePO_4$ cells. Regarding solid electrolytes, gel polymer electrolytes can provide a tradeoff between high ionic conductivity and improved safety by encapsulating the liquid electrolyte within a polymeric network[5,6]. These encapsulated liquid electrolytes play a key role in ion transport and their components need to be carefully selected for an optimal set of properties[7].

Ionic liquids (ILs) are safer alternatives than conventional flammable organic solvents due to their low volatility, non-flammability and stability against superoxide radicals[8,9]. Pyrrolidinium and imidazolium cations and fluorine-based anions, such as bis(trifluoromethanesulfonyl)imide (TFSI), are the most recognized IL-based electrolytes[8,10-14]. However, a less well-known IL, N,N-diethyl-N-methyl-N-(2-methoxyethyl)ammonium bis(trifluoromethanesulfonyl)imide (DEME-TFSI), has shown promising properties in Li-O_2 cells, such as low polarization during galvanostatic cycling[15,16] and a good oxygen supply capacity for the oxygen reduction reaction[17]. Beyond the use of advanced catalysts to assist the oxygen evolution reaction (OER)/oxygen reduction reaction (ORR) kinetics[18,19], a method to seek higher performance is to increase the fluorine content within the electrolyte structure, as it has a beneficial effect in the formation of a passivating lithium protection layer[20] and/or a tendency to increase oxygen solubility in the solution (the active material in this type of cell)[17]. A relatively easy method to increase the fluorine content in IL-based electrolytes is by tuning their anions and/or cations[21,22]. In contrast, the use of ILs in gel polymer electrolytes, typically known as iongels, is becoming increasingly more common[21] but has not been largely explored for Li-O_2 cells. For example, Zhao *et al.* developed an ultraviolet (UV)-cured iongel containing a 1-ethyl-3-methylimidazolium tetrafluoroborate IL, dimethyl sulfoxide and LiTFSI, encapsulated in a polymer matrix formed by poly(methyl methacrylate) (PMMA) and *a* triacrylate[23]. Symmetrical lithium cells containing this iongel presented an overpotential of < 0.1 V for 130 h when cycled at 0.3 $mA{\cdot}h^{-1}$. Other approaches involved the use of poly(vinylidene fluoride-co-hexafluoropropylene), a pyrrolidinium-based IL and LiTFSI[24,25] or PMMA as the polymeric matrix[26].

In this work, we present a study of highly conductive iongel electrolytes based on five different ILs designed to improve the Li^+ transport properties and electrochemical performance of Li-O_2 cells. The $[DEME]^+$ cation and $[TFSI]^-$ anion are tuned to increase the presence of fluorine moieties with a highly delocalized charge. The synergy between the cations and anions of the IL and the corresponding lithium salts is explored. The preparation of iongels soft solid electrolytes by fast photopolymerization methods is then pursued. The mechanical, thermal and electrochemical properties of the obtained iongels are investigated with particular attention devoted to the optimization of the ionic conductivity. These soft solid iongel electrolytes are first tested against lithium metal electrodes in symmetrical cells and compared to their liquid electrolyte analogs. Finally, their performance in Li-O_2 cells with both solid and IL electrolytes is evaluated.

RESULTS AND DISCUSSION

Synthesis and characterization of ILs and iongels

In this work, four fluorinated ILs, as alternatives to the commercially available DEME-TFSI IL, were designed to optimize Li-O_2 cell performance [Figure 1]. The $[TFSI]^-$ anion of DEME-TFSI was replaced by different anions, namely, bis(fluorosulfonyl)imide $[FSI]^-$, bis(perfluoroethylsulfonyl)imide $[BETI]^-$ and nonafluoro-1-butanesulfonate $[C_3F_9SO_3]^-$. The objective was to modify and increase the fluorinated moieties in the resultant IL and the ionicity of the different ILs with respect to DEME-TFSI. The cation of the DEME-TFSI IL, $[DEME]^+$, was redesigned to incorporate a fluorinated pendant group while maintaining most of its chemical structure (obtaining N,N-diethyl-N-methyl-N-((trifluoroethoxy) ethyl) ammonium, FD), following previous works[17]. The IL using this $[FD]^+$ cation was labeled as FD-TFSI, which was obtained commercially.

The $[DEME]^+$-based ILs with different anions were synthesized by a typical salt metathesis reaction [Scheme 1][17,27,28]. An anion exchange reaction was carried out between a $[Br]^-$ anion (from N,N-diethyl-N-methyl-N-(2-methoxyethyl)ammonium bromide, [DEME][Br]) and the negative ion of a commercially available monovalent salt (e.g., X^+Y^-, where $X^+ = Na^+$, Li^+ or K^+ and $Y^- = [TFSI]^-$, $[BETI]^-$ or $[C_3F_9SO_3]^-$). They were characterized by ^1H, ^{13}C and ^{19}F NMR, as described in the Supplementary Figure 1, as well as by attenuated total reflection Fourier transform infrared (FTIR) spectroscopy [Supplementary Figure 2]. DEME-TFSI was also synthesized and compared to a commercial version of this IL to prove the viability of the synthesis method [Supplementary Figure 2A]. DEME-Br presented one broadband in the FTIR spectrum at 3450 and 1630 cm^{-1} corresponding to water and O-H bending[29], respectively, which disappeared in the DEME-TFSI spectrum. The bands between 3000 and 2800 cm^{-1} were assigned to the stretching vibrations of the C-H bonds of the alkyl chain of the $DEME^+$ cation[30]. The characteristic bands of the fluorinated $TFSI^-$ anion appeared in the DEME-TFSI spectrum at 651, 741 and 762 cm^{-1} (attributed to S-N-S symmetric and asymmetric stretching, respectively), 1134 and 1346 cm^{-1} (-SO_2 asymmetric stretching), 1058 and 790 cm^{-1} (-C-S- stretching) and 1165 cm^{-1} (C-F_3 asymmetric stretching)[30]. Similar bands were observed for DEME-BETI. In contrast, DEME-FSI presented the characteristic bands of the [FSI]- anion at 1218 and 1365-1383 cm^{-1} (attributed to -SO_2 symmetric and asymmetric stretching, respectively), 572 cm^{-1} (δ_{ip} (O_2S-N-SO_2) + ν(S-F) + δ_{ip}(SO_2-F)) and 454-482 cm^{-1} (δ_{sci} (SO-F) + δ (OS-N-SO-) and δ_{sci} (SO-F) + δ_{op} (O_2S-F), respectively)[30]. DEME-$C_3F_9SO_3$ presented the characteristic bands of the $[C_3F_9SO_3]$- anion at 638, 1225 and 518, 1261, 1281 cm^{-1} (attributed to -SO_3 symmetric and asymmetric stretching, respectively) and 755 cm^{-1} (C-F_3 symmetric stretching)[30].

These ILs were further analyzed via differential scanning calorimetry. As shown in Supplementary Figure 3A-C, DEME-BETI and DEME-$C_3F_9SO_3$ presented small endothermic peaks at -40.5 and -22.1 °C, respectively. The DEME-FSI and DEME-TFSI thermograms were flat, suggesting that their melting temperatures are probably below -80 °C, outside the equipment range or nonexistent. Literature works claim only Tg transitions at -94.2 and -111.4 °C for DEME-TFSI and DEME-FSI, respectively[31]. Hence, all the ILs are liquid at room temperature, which is a desirable property from a practical battery perspective.

Regarding the diffusion properties, the mobility of the ions within an electrolyte is directly proportional, amongst other properties, to the viscosity of the system[32]. Thus, the dynamic viscosity of these ILs was measured at 25 and 60 °C [Supplementary Figure 3D]. As expected, the viscosity decreased with temperature (e.g., up to four times lower at 60 °C for DEME-$C_3F_9SO_3$) and the DEME-FSI IL possessed the lowest values of 71.1 and 26.6 mPa·s at 25 and 60 °C, respectively. The viscosity of an IL is usually determined by its hydrogen and/or van der Waals forces and is usually affected by the ion size, branching

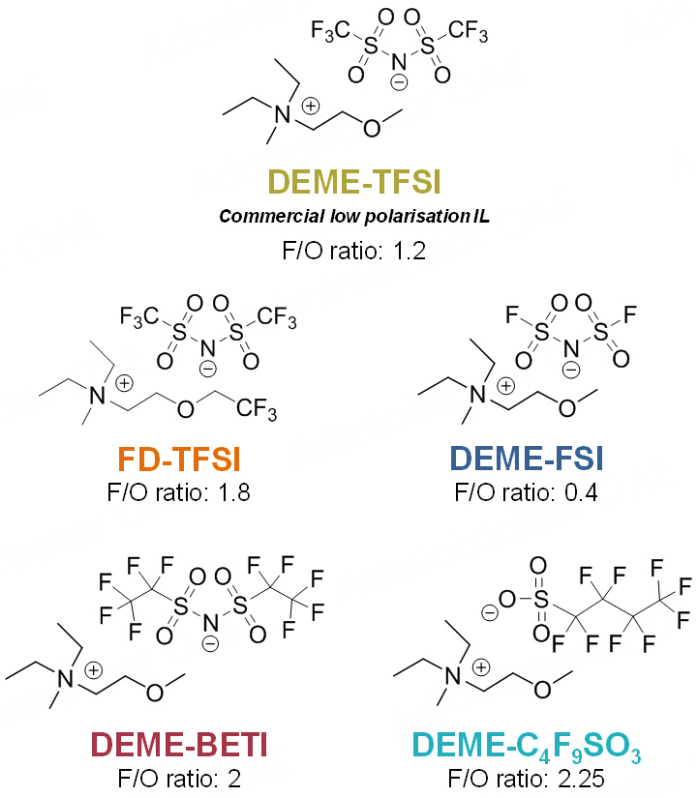

Figure 1. Chemical structures of the ILs evaluated in this work. ILs: Ionic liquids.

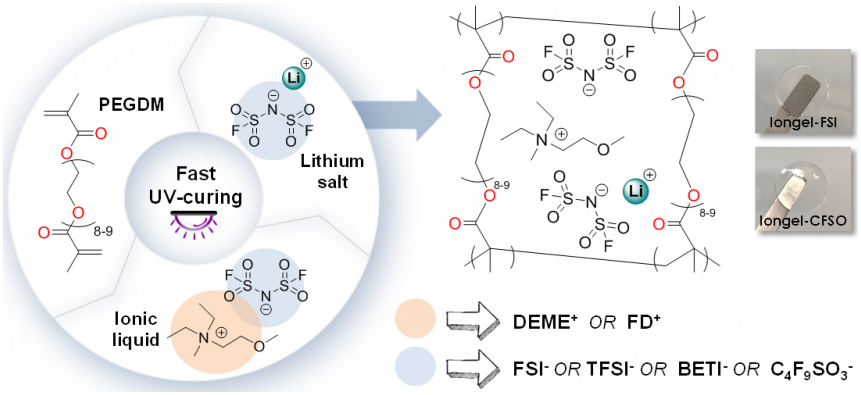

Scheme 1. Schematic of UV-photopolymerisation process to obtain crosslinked iongel electrolytes.

and/or functional groups[8]. The additional fluorinated moieties of DEME-BETI, DEME-$C_3F_9SO_3$ and FD-TFSI increased the ion sizes, leading to an increase in viscosity. Interestingly, DEME-BETI and FD-TFSI had similar F/O ratio (~2), but the viscosity of DEME-BETI at room temperature was double (319 compared to 144 mPa·s, respectively), suggesting that FD-TFSI has ions with weaker interaction forces, leading to smaller energies being required for molecular motion.

Scheme 1 shows the simple UV-photopolymerisation method followed to obtain iongels with very high liquid electrolyte contents (up to 90 wt.%)[16]. Poly(ethylene glycol) dimethacrylate (PEGDM) was directly mixed with the ionic liquid electrolyte (ILE) in the presence of a radical photoinitiator (2-hydroxy-2-

methylpropiophene). After UV irradiation for < 2 min on the drop-cast solution, self-standing and transparent membranes were obtained. In all cases, the LiTFSI salt was dissolved in the ILs to form the ILEs, which were labeled as Iongel-xx*, where xx is the anion of the IL selected and * corresponds to the use of LiTFSI as the salt (e.g., Iongel-FSI*, where DEME-FSI and LiTFSI were used as the ILE) [Table 1, Supplementary Table 1]. In addition to LiTFSI, other salts, such as lithium bis(fluorosulfonyl)imide (LiFSI), lithium bis(perfluoroethylsulfonyl)imide (LiBETI) and lithium nonafluoro-1-butanesulfonate ($LiC_3F_9SO_3$), were also used, as shown in Table 1. In all cases, the degree of crosslinking was monitored via FTIR spectroscopy and conversions of ≥ 94% were reached [Supplementary Figure 4]. The monomer conversion was examined through the C=C stretching vibration of the acrylic groups (1640-1635 cm^{-1}), which significantly decreased/disappeared after UV irradiation[33].

The thermal and mechanical stability of the iongels was evaluated via thermal gravimetrical analysis (TGA) and dynamic mechanical thermal analysis (DMTA). From a thermal perspective [Figure 2A], all membranes using the LiTFSI salt (except for Iongel-FSI*) behaved very similarly and did not present any thermal degradation until ~310-330 °C. This remarkably high thermal stability was directly attributed to the intrinsic properties of the ILs (e.g., a decomposition temperature of ~325 °C for DEME-TFSI and low volatility)[17]. From this temperature, a one-step degradation occurred for all the iongels analyzed. The thermogram of Iongel-FSI* showed an earlier thermal decomposition than the other membranes. This was attributed to the lower stability of the FSI^- anion compared to the $TFSI^-$ anion[31]. In summary, all iongel membranes are very stable from a thermal perspective, well above typical lithium battery operating conditions (< 100 °C)[34].

From a mechanical perspective, the iongels containing the LiTFSI salt were first evaluated [Supplementary Figure 5A]. Overall, the membranes kept their modulus between 10^4 and 10^5 Pa at different temperatures (from 0 to 100 °C), illustrating their mechanical stability at high temperatures. Interestingly, the iongels containing the same anionic group in the salt and IL showed a higher modulus (i.e., ~10^5 Pa for Iongel-TFSI* and Iongel-FD*, both containing $TFSI^-$ anions). Subsequently, Iongel-FSI*, Iongel-BETI* and Iongel-CFSO* were reformulated by adding LiFSI, LiBETI and $LiC_3F_9SO_3$ salts, respectively, at a 20 mol.% concentration and tested [Figure 2B]. The results showed an improvement from 2 × 10^4 to 4 × 10^4 Pa for Iongel-FSI, from 4 × 10^4 to 10^5 Pa for Iongel-BETI and from 4 × 10^4 to 6 × 10^4 Pa for Iongel-CFSO. Furthermore, iongels containing the fluorinated cation (FD-TFSI) at lower ILE contents in the iongel formulation were also assessed [Supplementary Figure 5B]. The results showed that, as expected, larger contents of polymer in the iongel formulation led to a higher modulus. In contrast, according to the Tan δ derivative, the iongels with a smaller anion presented a lower Tg transition, thereby positively enhancing Li^+ transport[35]. Hence, the ranking in terms of Tg was Iongel-FD (-54.1 °C) < Iongel-FSI (-49.7 °C) < Iongel-TFSI (-43.2 °C) < Iongel-CFSO (-41 °C) < Iongel-BETI (-26.5 °C). Overall, the low Tg of these iongels, together with their high thermal and mechanical stability, make these polymer electrolytes interesting materials for further investigation.

Next, the ionic conductivity (σ) of the iongels containing the LiTFSI salt was evaluated by electrochemical impedance spectroscopy (EIS) [Figure 3A]. Iongel-FD had the highest σ value (2.48 × 10^{-3} S·cm^{-1} at 25 °C), very close to its liquid counterpart (3.24 × 10^{-3} S·cm^{-1} at 25 °C, Figure 3C). Similar to the DMTA results, iongels containing the same anionic group in the salt and IL seemed to have higher conductivities. Consequently, the Iongel-FSI, Iongel-BETI and Iongel-CFSO membranes were further investigated [Figure 3B]. A significant improvement was found for the Iongel-CFSO and Iongel-FSI formulations, with the latter having the highest conductivity of the group (7.8 × 10^{-3} S·cm^{-1} at 25 °C). To the best of our knowledge, this value is one of the highest ionic conductivities reported in the literature for IL-based solid electrolytes. In the case of Iongel-BETI, the ionic conductivity was very similar in both cases

Table 1. Iongel electrolyte compositions containing 90 wt.% liquid electrolyte and 10 wt.% PEGDM crosslinker

Sample	Liquid electrolyte[a]	
	IL	Salt
Iongel-FSI*	DEME-FSI	LiTFSI in all cases
Iongel-TFSI* or Iongel-TFSI	DEME-TFSI	
Iongel-FD* or Iongel-FD	FD-TFSI	
Iongel-BETI*	DEME-BETI	
Iongel-CFSO*	DEME-$C_3F_9SO_3$	
Iongel-FSI	DEME-FSI	LiFSI
Iongel-BETI	DEME-BETI	LiBETI
Iongel-CFSO	DEME-$C_3F_9SO_3$	$LiC_3F_9SO_3$

[a]At a 20 mol.% concentration of the selected salt. PEGDM: Poly(ethylene glycol) dimethacrylate.

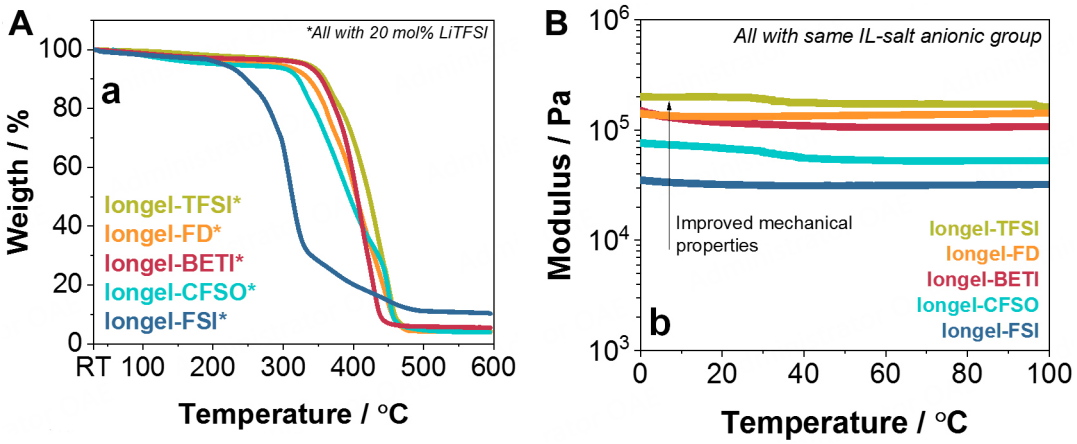

Figure 2. (A) TGA thermograms from room temperature to 600 °C of the iongel membranes and (B) DMTA at compression from 0 to 100 °C of iongel membranes containing 20 mol.% of a lithium salt with the same anion as the ILE. TGA: Thermal gravimetrical analysis; DMTA: dynamic mechanical thermal analysis; ILE: ionic liquid electrolyte.

(~1.2 × 10^{-3} S·cm^{-1} at 25 °C). Despite having higher chemical compatibility, the ionic conductivity might not have improved due to the potentially higher viscosity of this electrolyte ($BETI^-$ > $TFSI^-$ size). Overall, the order of the ionic conductivities was Iongel-FSI > Iongel-FD-TFSI > Iongel-BETI ~ Iongel-TFSI > Iongel-CFSO. The fluorinated moieties were targeted to increase oxygen solubility in the electrolyte, which has a beneficial effect on Li-O_2 cells[17]. However, in addition, these groups are usually used to promote delocalization of the anionic charge due to their electron-withdrawing capacity, thereby improving Li^+ mobility[36]. Hence, iongels containing a higher fluorine content showed higher ionic conductivity, except for the Iongel-CFSO class, possibly due to their much higher/lower viscosity. The same study was carried out for comparison using the ILEs containing LiTFSI or their analogous salts [Supplementary Figure 6A, Figure 3C]. It can be concluded that it is possible to achieve conductivities of the same order of magnitude as liquid electrolytes with iongel solid electrolytes.

Furthermore, a small study was carried out with Iongel-FD [Supplementary Figure 6B], in which increasing weight ratios of the ILE led to higher ionic conductivities. Due to these results, only cells with electrolytes (either iongel or liquid electrolytes) containing the same anionic group in the salt and IL were further evaluated. Furthermore, the ionic conductivities increased linearly with temperature and followed

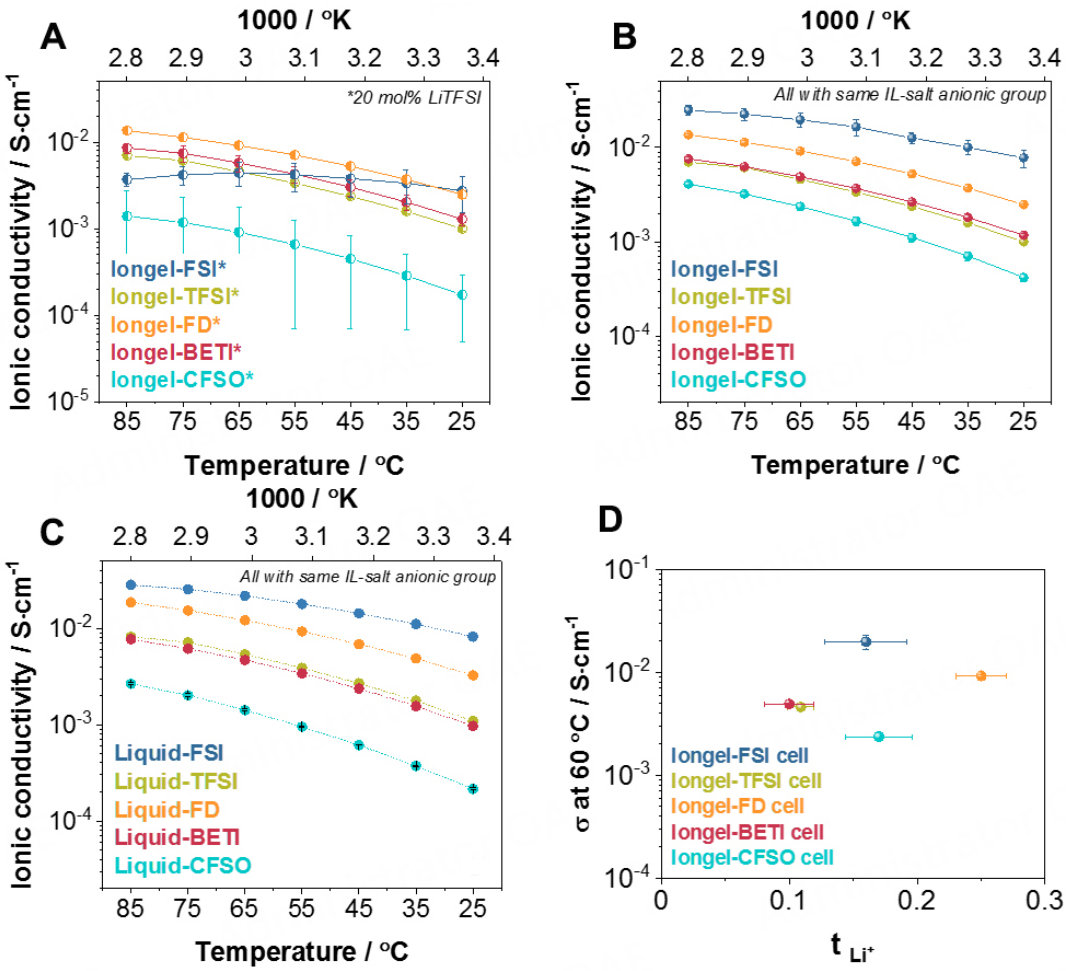

Figure 3. Ionic conductivities obtained by EIS measurements at different temperatures of cells using (A) Iongel-XX* electrolytes containing 20 mol.% LiTFSI, (B) Iongel-XX electrolytes containing 20 mol.% of a lithium salt with the same anionic group as the ILE and (C) liquid electrolytes containing 20 mol.% of a lithium salt with the same anionic group as the ILE. (D) Ionic conductivities at 60 °C versus their lithium transference number. EIS: Electrochemical impedance spectroscopy; ILE: ionic liquid electrolyte.

Arrhenius-type thermally activated behavior[37,38]:

$$\sigma = \sigma_o \cdot e^{\left(\frac{-E_a}{kT}\right)} \quad (1)$$

where σ_o is the pre-exponential factor, E_a is the activation energy and k is the Boltzmann constant. The effect of the selected anion on the ion transport mechanism was also evidenced in the trend observed for the activation energies [Supplementary Figure 6C]. Iongel-CFSO presented the highest value (0.35 eV), possibly due to its poor Li^+ solvation ability and significant presence of electron-withdrawing groups (high F/O ratio of DEME-$C_3F_9SO_3$ IL of 2.25) to the detriment of Li^+ mobility coordinating groups (i.e., the sulfonyl functional group)[39]. This is in accordance with results found in the literature[40], in which it has been proved that Li^+ is mainly coordinated by the oxygen atoms of the anions in ILs. This activation energy was significantly reduced for Iongel-FSI (0.18 eV). In this case, the F/O was the lowest of the group (0.4), having a dominant presence of Li^+ coordinating structures favoring ion mobility. More interestingly, the results showed that, in all cases, the activation energy was lower in the iongel electrolytes than in the liquid electrolytes (e.g., 0.31 eV compared to 0.28 eV for Liquid-BETI and Iongel-BETI, respectively). It is possible

that the low Tg of the iongels and the presence of ethylene oxide segments within the polymeric network might favor lower activation energies as they provide additional ion mobility pathways to the system (stable complexes of Li^+ with the ether oxygens)[41].

The contribution of ionic conductivity exclusively resulting from Li^+ was evaluated through the determination of the lithium transference number (t_{Li+}), according to the well-known Evans-Vincent-Bruce method [Supplementary Figure 7]. The analysis of the iongel electrolytes [Figure 3D] revealed that t_{Li+} ranged between 0.10 and 0.25, in accordance with values found in the literature[8,39,42]. Iongel-BETI and Iongel-TFSI had the lowest values (~0.10). TFSI-based IL has been reported to form Li^+ -$[TFSI^-]_2$ negative ion pairs, which does not favor ion mobility under an electric field, thus lowering the t_{Li+} of the electrolyte[39]. In contrast, the poorer Li^+ solvation ability of DEME-$C_3F_9SO_3$ might lead to a t_{Li+} discreet promotion, comparable to the Iongel-FSI value (~0.17). The Iongel-FD electrolyte had the highest t_{Li+} (0.25). Overall, the iongels developed in this work possess, to our knowledge, some of the highest ionic conductivity values found in the literature[8,43-45] and have suitable ion conductive properties for battery applications. Furthermore, it has been demonstrated that, through the designed ILs, it is possible to achieve superior ionic conductivities than the more studied [DEME][TFSI]-based electrolytes.

Symmetrical lithium cells

Symmetrical lithium cells containing the iongels were assembled within two lithium metal foils inside a glove box to determine their stability against lithium. Current densities were increased from 0.01 to 2 $mA{\cdot}cm^{-2}$ and cells were cycled three times for each current (1 h half-cycle). The average potential (absolute value) achieved at each current rate is plotted in Figure 4A. The results showed that the electrolytes with smaller anion sizes led to lower overpotentials, with cells having a critical current density (where E_{WE} exceeds 1 V) of 0.5 $mA{\cdot}cm^{-2}$ for Iongel-TFSI (0.33 V) and an excellent 2 $mA{\cdot}cm^{-2}$ for Iongel-FSI (0.97 V). This trend was also found in equivalent cells based on liquid electrolytes [Supplementary Figure 8A] but with slightly lower overpotentials (e.g., 0.21 V for Liquid-TFSI at 0.5 $mA{\cdot}cm^{-2}$). At relatively lower and usually reported current rates (i.e., 0.1 $mA{\cdot}cm^{-2}$) in literature, the iongel cells exhibited a wide range of overpotentials with the order of Iongel-FSI (20 mV) < Iongel-TFSI (45 mV) < Iongel-FD (87 mV) < Iongel-BETI (0.41 V) < Iongel-CFSO (2.9 V). The same tendency was found in cells with liquid electrolytes, with overpotentials ranging from as low as 9 mV (Liquid-FSI), 50 mV (Liquid-TFSI) and 60 mV (Liquid-BETI).

Due to these promising results, symmetrical lithium cells with DEME-TFSI- and DEME-FSI-based electrolytes were further cycled (1 h platting and 1 h stripping) in galvanostatic mode at 0.5 $mA{\cdot}cm^{-2}$ [Figure 4B]. Cells with the Iongel-FSI electrolyte showed a polarization as low as 60 mV for 50 h, suggesting good compatibility between lithium metal and the iongel. On the opposite side, cells with the Iongel-TFSI electrolyte suffered from dendritic growth in a much earlier step, leading to a "soft" short circuit until the final hard-short circuit after 23 h[46]. The same trend was found in equivalent cells with liquid electrolytes [Supplementary Figure 8B]. Cells with the Liquid-TFSI electrolyte had lower overpotentials (0.17 V), but they increased rapidly after 14 h of cycling. Cells containing the Liquid-FSI electrolyte had a polarization as low as 41 mV for at least 100 h. Hence, in comparison with the Iongel-TFSI electrolytes, the Iongel-FSI membranes were able to potentially suppress dendritic growth more efficiently and cycling was further pushed to current densities of 1 $mA{\cdot}cm^{-2}$ [Figure 4C] and 2 $mA{\cdot}cm^{-2}$ [Figure 4D]. At 1 $mA{\cdot}cm^{-2}$, the cells showed overpotentials of < 0.40 V for 45 h, which increased smoothly with cycling. The stripping/plating profiles became sharper and less homogeneous under 2 $mA{\cdot}cm^{-2}$ (polarization ranging from 0.6 to 1.1 V) until the distinctive fingerprint of a short-circuited cell appeared after 41 h[47].

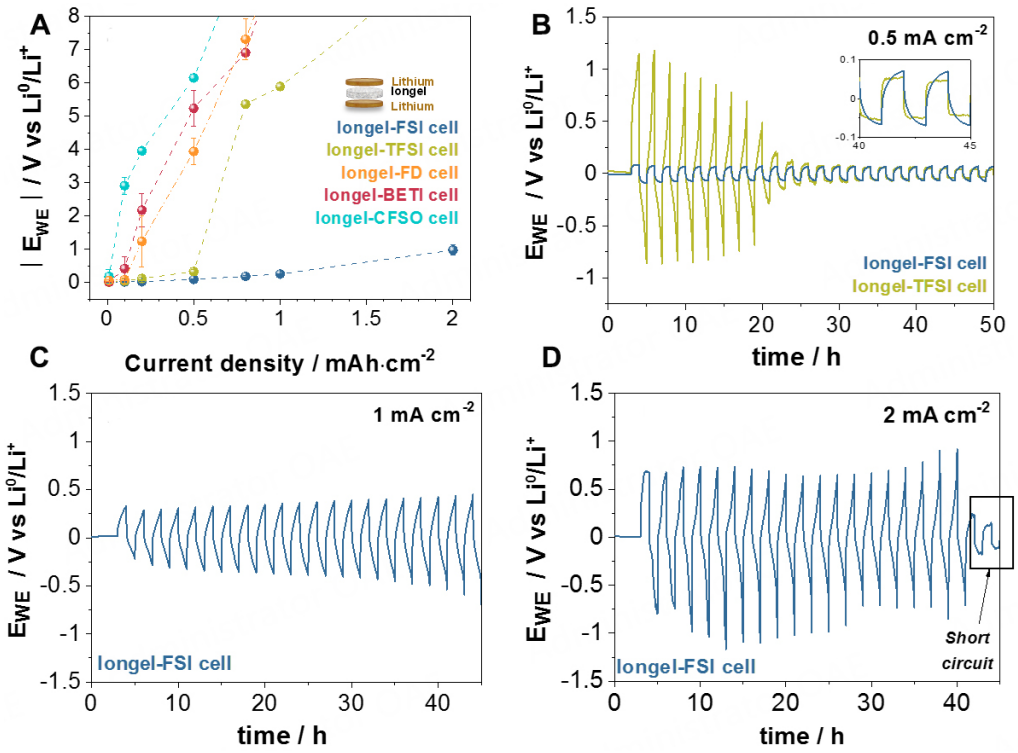

Figure 4. Galvanostatic tests on symmetrical lithium cells at 60 °C. (A) Average potentials achieved at each current density from 0.01 to 2 mA·cm^{-2}. Each current cell was cycled three times with a 1 h break. Long galvanostatic cycling at (B) 0.5, (C) 1 and (D) 2 mA·cm^{-2}.

The outstanding performance of cells with FSI$^-$-based electrolytes compared to the other systems could be related to the interaction of these electrolytes with lithium metal. It is well known that a passivating organic-inorganic SEI is spontaneously formed at the electrolyte-lithium metal interphase from the decomposition products of the electrolyte, including LiF, LiCl and Li_2O or Li_2CO_3[48,49]. Therefore, it is usually desired that the electrolyte contains at least one SEI precursor, such as LiTFSI or LiFSI[48]. Actually, some reports in the literature have presented remarkable results on symmetrical cells when FSI$^-$ anions are used within the electrolyte, relating them with the formation of a SEI rich in LiF[42,50]. This could potentially explain the superior performance of our FSI$^-$ based electrolytes. In order to elucidate further the platting/stripping behavior of cells using Liquid-FSI at their current boundary limits [Supplementary Figure 8C], impedance measurements were performed before (EIS-0) and after cycling at 2 mA·cm^{-2} (EIS-2). The Nyquist plots are shown in Supplementary Figure 8D. As observed, the electrolyte and interfacial contribution resistances showed a negative evolution over cycling. This decrease in resistance represents a typical behavior of a recoverable soft short-circuit[47], in which the cell was able to keep cycling to the detriment of the electrolyte and SEI stability. The characteristic frequencies ($fc = {}^{1}/_{2\pi RC}$) of the interphase and electrolyte shifted from 1.38 and 486 Hz to 7.93 and 5430 Hz, respectively, suggesting a change in the composition (potential degradation) of these materials at 2 mA·cm^{-2}[51]. Overall, it is noteworthy that these cycling results reveal the possible use of Iongel-FSI as an effective electrolyte/anolyte material for lithium protection.

Prior to Li-O_2 battery testing, Li^0//stainless steel cells were prepared and scanned at 0.2 mV·s^{-1} to investigate the upper stability window of the studied liquid electrolytes [Supplementary Figure 9]. The best stability window values were 4.77-4.92 V for TFSI$^-$ containing electrolytes (Liquid-TFSI and Liquid-FD cells, respectively) and ~3.2-3.6 V for the rest of the cells. Following these results, cut-off potentials of 2.0 and 3.6 V were established for Li-O_2 cycling.

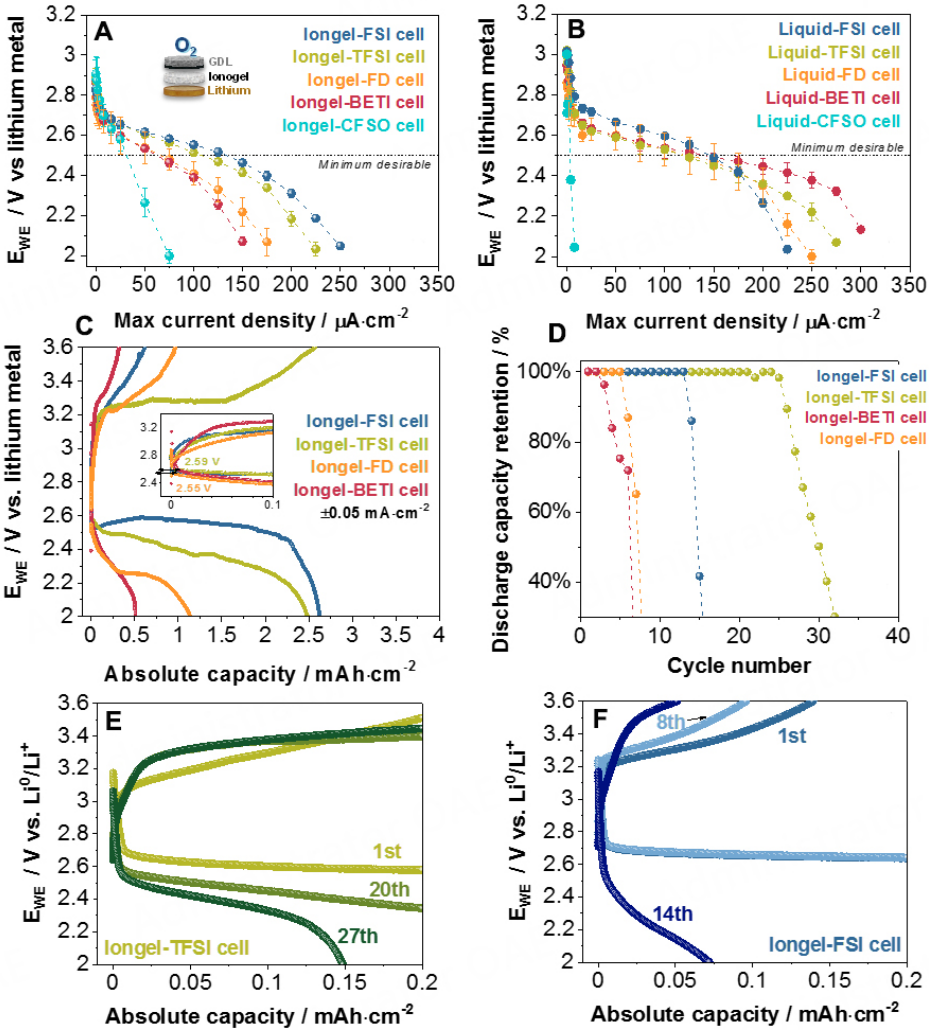

Figure 5. Cycling of Swagelok Li-O_2 cells at 60 °C. (A and B) Potential against current density, where the potential plotted is the average potential of the cell reached at each current density during a dynamic discharge (three cell average). (C) Discharge-charge profiles at 0.05 mA·cm^{-2} and galvanostatic cycling at ± 0.05 mA·cm^{-2} with limited capacity (0.2 mAh·cm^{-2}). (D) Discharge capacity retention. Selected potential profiles of (E) Iongel-TFSI and (F) Iongel-FSI cells.

Li-O_2 cells

First, a C-rate test (dynamic discharge) was undertaken on Swagelok Li-O_2 cells to determine the average steady potentials achieved at different current densities (from 5 μA·cm^{-2} to 0.35 mA·cm^{-2} with 15 min/per rate). The results were heterogeneous [Figure 5A]. Cells with Iongel-FSI and Iongel-TFSI could be cycled at higher current rates (up to 0.1 mA·cm^{-2}), whereas cells with Iongel-FD and Iongel-BETI achieved more modest values (~60 μA·cm^{-2}). Cells with Iongel-CFSO electrolytes exhibited a dramatic drop in the cell potential beyond the 25 μA·cm^{-2} current rate, matching the poorer performance shown previously in the symmetrical lithium cells. Despite containing a higher fluorine content, the viscosity of the system might play a more dominant role, limiting the mobility of the Li^+ toward the positive cathode. Cells with liquid electrolytes were also evaluated for comparison [Figure 5B] and all of them, with the exception of the Liquid-CFSO electrolyte, exhibited a more homogenous performance with a stable discharge potential until a 0.12 mA·cm^{-2} current rate. Considering the results obtained for cells using iongel electrolytes, 50 μA·cm^{-2} was selected as the current density for further galvanostatic testing with an average discharge potential of ~2.6 V. Due to their low performance, Iongel-CFSO electrolytes were not further tested.

Subsequently, Li-O_2 cells with iongel electrolytes were fully discharged/charged at ±50 μA·cm^{-2} and 60 °C between 2.0 and 3.6 V *vs*. Li^0/Li^+ after 3 h of conditioning at the OCV [Figure 5C]. Similar to the rate tests, the electrolytes could be divided into two groups: Iongel-FSI and Iongel-TFSI electrolytes [with cells giving the highest discharge capacities (2.62 and 2.48 mAh·cm^{-2}, respectively)] and Iongel-FD and Iongel-BETI (with cells showing a sharp potential decay at the beginning of the discharge and 0.5 and 1.14 mAh·cm^{-2} discharge capacities, respectively). Furthermore, the onset potential for the ORR on the discharge process was observed at 2.55-2.59 V *vs*. Li^0/Li^+ for all the cells, close to the value anticipated on the rate test (2.60 V *vs*. Li^0/Li^+). In contrast, Li-O_2 cells with liquid electrolytes [Supplementary Figure 10A] exhibited cleaner profiles with absolute discharge capacities between 2.5 and 3.0 mAh·cm^{-2}. As anticipated for the rate test, ORR potentials were observed between 2.65 and 2.72 V *vs*. Li^0/Li^+ for all the cells, where cells with the Liquid-FSI electrolyte showed the highest values (3 mAh·cm^{-2} discharge capacity and 2.72 V *vs*. Li^0/Li^+ ORR potential). Overall, Li-O_2 cells based on the FSI^- anion were the most promising systems.

Finally, Li-O_2 cells were cycled with limited capacity (0.2 mA·cm^{-2}) at 50 μA·cm^{-2} and a potential window of 2.0-3.6 V. Figure 5D displays the discharge capacity retention of the three iongel cells. The best Li-O_2 cell had Iongel-TFSI as an electrolyte and cycled for 25 cycles at 100% Coulombic efficiency [Figure 5E]. In contrast, cells with the Iongel-FSI electrolyte were able to cycle 13 times at 100% capacity retention but with lower charge capacities than cells with Iongel-TFSI [Figure 5F]; afterward, the cell potential drastically faded. Cells using Iongel-FD and Iongel-BETI electrolytes had poorer cycling performance (five and two cycles, respectively), in accordance with the poorer results obtained on the full discharge/charge cycling. Their potential profiles are shown in Supplementary Figure 10C and D. Cells with ILEs were also examined [Supplementary Figure 10B] and surprisingly, their cycling performance was equivalent to the cells with iongel electrolytes. Actually, the number of cycles at 100% discharge capacity retention was the same for both cells using polymer and liquid electrolytes, except for $TFSI^-$-based electrolytes, in which they decreased from 25 to 10 cycles before drastic capacity fading. Overall, the FSI^-- and $TFSI^-$-based electrolytes were the best for Li-O_2 cell tests in terms of capacity and cycling capability. Despite having a larger fluorinated content, Iongel-CFSO, Iongel-BETI and Iongel-FD did not improve the performance in Li-O_2 cells. The higher viscosity of these systems had a major impact on their battery performance.

CONCLUSIONS

In this work, we presented a whole new family of polymeric iongel electrolytes based on the tailored design of ILs that are suitable for Li-O_2 cells. Four ILs were synthesized by combining different cations and anions, all of them variations of the DEME-TFSI IL. A fast UV-photopolymerization process was used to obtain transparent and flexible iongels with very high liquid electrolyte contents (up to 90 wt.%). Due to the presence of the IL electrolytes, these iongels were exceptionally stable from a thermal perspective (no degradation observed up to ~310 °C). Mechanical tests showed sufficient robustness for battery cell operation (~10^5 Pa).

Regarding ionic conductivity, electrolytes using analogous counterions between the salt and the IL showed higher values and followed the order of Iongel-FSI > Iongel-FD > Iongel-BETI ~ Iongel-TFSI > Iongel-CFSO, potentially due to the higher viscosity of the ILEs containing larger anions. In addition, the iongels showed conductivity values comparable to the liquid electrolytes and, to the best of our knowledge, we show here one of the highest ionic conductivities reported in the literature for iongel electrolytes (7.8×10^{-3} S·cm^{-1} at 25 °C, Iongel-FSI). Furthermore, this iongel electrolyte showed excellent performance in symmetrical lithium cells, with cells being able to cycle at 2 mA·cm^{-2}, a current density well above the ones usually reported in the literature. Moreover, the iongel was able to slow dendritic growth more efficiently compared to its liquid counterpart and the other iongels analyzed in this work (having critical current densities of

0.5 mA·cm^{-2}). When Li-O_2 cells were cycled, cells with Iongel-TFSI exhibited one of the highest absolute discharge capacities (2.48 mAh·cm^{-2}) and excellent cycling capability with 100% capacity retention and 100% Coulombic efficiency for at least 25 cycles. In general, the FSI^- and $TFSI^-$ based electrolytes were the best for Li-O_2 cell tests in terms of capacity and cycling capability. Iongel-CFSO, Iongel-BETI and Iongel-FD had a lower performance despite their larger fluorinated content.

Overall, the findings of this work show the potential use of polymeric iongels as electrolytes in lithium rechargeable cells. Due to their remarkable lithium compatibility, these soft solid ionic materials could also be used for effective lithium protection. In addition, the simplicity of the photopolymerization approach brings advantages for easier adoption for industrial batteries.

DECLARATIONS

Author's contributions

Conceptualization: Alvarez-Tirado M, Castro L, Tomé LC, Mecerreyes D
Data curation, investigation, validation and visualization: Alvarez-Tirado M
Formal analysis: Alvarez-Tirado M, Castro L, Guzmán-González G, Guéguen A, Mecerreyes D
Methodology: Alvarez-Tirado M, Guzmán-González G, Tomé LC, Mecerreyes D
Writing - original draft and review & editing: Alvarez-Tirado M, Castro L, Guzmán-González G, Guéguen A, Tomé LC, Mecerreyes D
Supervision: Castro L, Mecerreyes D
Ionic liquids: Tomé LC
Funding acquisition: Mecerreyes D

Availability of data and materials

The experimental details are provided in the Supplementary Material.

Financial support and sponsorship

This work was supported by the Horizon 2020 European Commission's funded Marie Skłodowska-Curie project POLYTE-EID [grant numbers 765828]. The manuscript was written through the contributions of all authors that have given approval to the final version of the Letter.

Conflicts of interest

All authors declared that there are no conflicts of interest.

Ethical approval and consent to participate

Not applicable.

Consent for publication

Not applicable.

REFERENCES

1. Ma L, Yu T, Tzoganakis E, et al. Fundamental understanding and material challenges in rechargeable nonaqueous Li-O_2 batteries: recent progress and perspective. *Adv Energy Mater* 2018;8:1800348. DOI
2. Grande L, Paillard E, Hassoun J, et al. The lithium/air battery: still an emerging system or a practical reality? *Adv Mater* 2015;27:784-800. DOI PubMed
3. Liu DH, Bai Z, Li M, et al. Developing high safety Li-metal anodes for future high-energy Li-metal batteries: strategies and

perspectives. *Chem Soc Rev* 2020;49:5407-45. DOI PubMed

4. Chen J, Li D, Lin K, Ke X, Cheng Y, Shi Z. Building a stable artificial solid electrolyte interphase on lithium metal anodes toward long-life Li-O_2 batteries. *J Power Sources* 2022;540:231603. DOI
5. Wang D, Mu X, He P, Zhou H. Materials for advanced Li-O_2 batteries: explorations, challenges and prospects. *Mater Today* 2019;26:87-99. DOI
6. Zhou D, Shanmukaraj D, Tkacheva A, Armand M, Wang G. Polymer electrolytes for lithium-based batteries: advances and prospects. *Chem* 2019;5:2326-52. DOI
7. Wang Q, Wang H, Wu J, Zhou M, Liu W, Zhou H. Advanced electrolyte design for stable lithium metal anode: from liquid to solid. *Nano Energy* 2021;80:105516. DOI
8. Liu K, Wang Z, Shi L, Jungsuttiwong S, Yuan S. Ionic liquids for high performance lithium metal batteries. *J Energy Chem* 2021;59:320-33. DOI
9. Stettner T, Balducci A. Protic ionic liquids in energy storage devices: past, present and future perspective. *Energy Stor Mater* 2021;40:402-14. DOI
10. Long L, Wang S, Xiao M, Meng Y. Polymer electrolytes for lithium polymer batteries. *J Mater Chem A* 2016;4:10038-69. DOI
11. Knipping E, Aucher C, Guirado G, Aubouy L. Room temperature ionic liquids versus organic solvents as lithium-oxygen battery electrolytes. *New J Chem* 2018;42:4693-9. DOI
12. Yang Q, Zhang Z, Sun XG, Hu YS, Xing H, Dai S. Ionic liquids and derived materials for lithium and sodium batteries. *Chem Soc Rev* 2018;47:2020-64. DOI PubMed
13. Nakamoto H, Suzuki Y, Shiotsuki T, et al. Ether-functionalized ionic liquid electrolytes for lithium-air batteries. *J Power Sources* 2013;243:19-23. DOI
14. Osada I, de Vries H, Scrosati B, Passerini S. Ionic-liquid-based polymer electrolytes for battery applications. *Angew Chem Int Ed* 2016;55:500-13. DOI PubMed
15. Ulissi U, Elia GA, Jeong S, et al. Low-polarization lithium-oxygen battery using [DEME][TFSI] ionic liquid electrolyte. *ChemSusChem* 2018;11:229-36. DOI PubMed
16. Alvarez-tirado M, Castro L, Guéguen A, Mecerreyes D. Iongel soft solid electrolytes based on [DEME][TFSI] Ionic liquid for low polarization lithium-O_2 batteries. *Batteries Supercaps* 2022;5:e202200049. DOI
17. Vanhoutte G, Hojniak SD, Bardé F, Binnemans K, Fransaer J. Fluorine-functionalized ionic liquids with high oxygen solubility. *RSC Adv* 2018;8:4525-30. DOI PubMed PMC
18. Li D, Zhang Q, Shen Z, et al. 3D hexapod-shaped Co-ZIFs-S derived co nanoparticles embedded into nitrogen and sulfur co-doped carbon decorated with ruthenium nanoparticles as efficient catalyst for rechargeable lithium oxygen battery. *Nano Energy* 2022;91:106644. DOI
19. Liu Y, Cai J, Zhou J, et al. Tailoring the adsorption behavior of superoxide intermediates on nickel carbide enables high-rate Li-O_2 batteries. *eScience* 2022;2:389-98. DOI
20. Kwak WJ, Rosy, Sharon D, et al. Lithium-oxygen batteries and related systems: potential, status, and future. *Chem Rev* 2020;120:6626-83. DOI PubMed
21. Tomé LC, Porcarelli L, Bara JE, Forsyth M, Mecerreyes D. Emerging iongel materials towards applications in energy and bioelectronics. *Mater Horiz* 2021;8:3239-65. DOI PubMed
22. Zhao M, Wu B, Lall-ramnarine SI, et al. Structural analysis of ionic liquids with symmetric and asymmetric fluorinated anions. *J Chem Phys* 2019;151:074504. DOI PubMed
23. Zhao H, Liu X, Chi Z, et al. Designing a new-type PMMA based gel polymer electrolyte incorporating ionic liquid for lithium oxygen batteries with Ru-based Binder-free cathode. *Appl Surf Sci* 2021;565:150612. DOI
24. Jung KN, Lee JI, Jung JH, Shin KH, Lee JW. A quasi-solid-state rechargeable lithium-oxygen battery based on a gel polymer electrolyte with an ionic liquid. *Chem Commun* 2014;50:5458-61. DOI PubMed
25. Pan J, Li H, Sun H, et al. A lithium-air battery stably working at high temperature with high rate performance. *Small* 2018;14:1703454. DOI PubMed
26. Amanchukwu CV, Chang H, Gauthier M, Feng S, Batcho TP, Hammond PT. One-electron mechanism in a gel-polymer electrolyte Li-O_2 battery. *Chem Mater* 2016;28:7167-77. DOI
27. Gouveia ASL, Tomé LC, Lozinskaya EI, Shaplov AS, Vygodskii YS, Marrucho IM. Exploring the effect of fluorinated anions on the CO_2/N_2 separation of supported ionic liquid membranes. *Phys Chem Chem Phys* 2017;19:28876-84. DOI
28. Costa AJ, Soromenho MR, Shimizu K, et al. Density, thermal expansion and viscosity of cholinium-derived ionic liquids. *Chemphyschem* 2012;13:1902-9. DOI PubMed
29. Rajkumar T, Ranga Rao G. Synthesis and characterization of hybrid molecular material prepared by ionic liquid and silicotungstic acid. *Mater Chem Phys* 2008;112:853-7. DOI
30. Paschoal VH, Faria LFO, Ribeiro MCC. Vibrational spectroscopy of ionic liquids. *Chem Rev* 2017;117:7053-112. DOI PubMed
31. Gao X, Wu F, Mariani A, Passerini S. Concentrated ionic-liquid-based electrolytes for high-voltage lithium batteries with improved performance at room temperature. *ChemSusChem* 2019;12:4185-93. DOI PubMed PMC
32. Pal P, Ghosh A. Solid-state gel polymer electrolytes based on ionic liquids containing imidazolium cations and tetrafluoroborate anions for electrochemical double layer capacitors: Influence of cations size and viscosity of ionic liquids. *J Power Sources* 2018;406:128-40. DOI

33. Vijayakumar V, Anothumakkool B, Kurungot S, Winter M, Nair JR. In situ polymerization process: an essential design tool for lithium polymer batteries. *Energy Environ Sci* 2021;14:2708-88. DOI
34. Wang J, Zheng Q, Fang M, Ko S, Yamada Y, Yamada A. Concentrated electrolytes widen the operating temperature range of lithium-ion batteries. *Adv Sci* 2021;8:e2101646. DOI PubMed PMC
35. Olmedo-martínez JL, Porcarelli L, Alegría Á, Mecerreyes D, Müller AJ. High lithium conductivity of miscible poly(ethylene oxide)/methacrylic sulfonamide anionic polyelectrolyte polymer blends. *Macromolecules* 2020;53:4442-53. DOI
36. Guzmán-gonzález G, Ramos-sánchez G, Camacho-forero LE, González I. Charge delocalization on BO_4^- centers to improve conductivity on single lithium ion conducting polymer electrolytes: a computational/experimental approach. *J Phys Chem C* 2019;123:17686-94. DOI
37. Aziz SB, Woo TJ, Kadir M, Ahmed HM. A conceptual review on polymer electrolytes and ion transport models. *J Sci Adv Mater Dev* 2018;3:1-17. DOI
38. Singh VK, Shalu, Balo L, Gupta H, Singh SK, Singh RK. Solid polymer electrolytes based on Li^+/ionic liquid for lithium secondary batteries. *J Solid State Electrochem* 2017;21:1713-23. DOI
39. Cai Y, Zhang Q, Lu Y, Hao Z, Ni Y, Chen J. An ionic liquid electrolyte with enhanced Li^+ transport ability enables stable li deposition for high-performance Li-O_2 Batteries. *Angew Chem Int Ed* 2021;60:25973-80. DOI
40. Tong J, Wu S, von Solms N, et al. The effect of concentration of lithium salt on the structural and transport properties of ionic liquid-based electrolytes. *Front Chem* 2019;7:945. DOI PubMed PMC
41. Bennington P, Deng C, Sharon D, et al. Role of solvation site segmental dynamics on ion transport in ethylene-oxide based side-chain polymer electrolytes. *J Mater Chem A* 2021;9:9937-51. DOI
42. Periyapperuma K, Arca E, Harvey S, et al. Towards high rate Li metal anodes: enhanced performance at high current density in a superconcentrated ionic liquid. *J Mater Chem A* 2020;8:3574-9. DOI
43. Eshetu GG, Mecerreyes D, Forsyth M, Zhang H, Armand M. Polymeric ionic liquids for lithium-based rechargeable batteries. *Mol Syst Des Eng* 2019;4:294-309. DOI
44. Karuppasamy K, Theerthagiri J, Vikraman D, et al. Ionic liquid-based electrolytes for energy storage devices: a brief review on their limits and applications. *Polymers* 2020;12:918. DOI PubMed PMC
45. Ray A, Saruhan B. Application of ionic liquids for batteries and supercapacitors. *Materials* 2021;14:2942. DOI PubMed PMC
46. Chen Z, Kim G, Kim J, et al. Highly stable quasi-solid-state lithium metal batteries: reinforced $Li_{1.3}Al_{0.3}Ti_{1.7}(PO_4)_3$/Li interface by a protection interlayer. *Adv Energy Mater* 2021;11:2101339. DOI
47. Kang D, Hart N, Xiao M, P. Lemmon J. Short circuit of symmetrical li/li cell in li metal anode research. *Acta Physico Chimica Sinica* 2021;37:1-6. DOI
48. Peled E, Menkin S. Review-SEI: past, present and future. *J Electrochem Soc* 2017;164:A1703-19. DOI
49. Wang A, Kadam S, Li H, Shi S, Qi Y. Review on modeling of the anode solid electrolyte interphase (SEI) for lithium-ion batteries. *NPJ Comput Mater* 2018:4. DOI
50. Rakov DA, Chen F, Ferdousi SA, et al. Engineering high-energy-density sodium battery anodes for improved cycling with superconcentrated ionic-liquid electrolytes. *Nat Mater* 2020;19:1096-101. DOI PubMed
51. Frenck L. Study of a buffer layer based on block copolymer electrolytes, between the lithium metal and a ceramic electrolyte for aqueous lithium-air battery. Grenoble, France: Universite Grenoble Alpes, 2016.